applied sciences

MDPI

Review

NiO-Based Electronic Flexible Devices

Marilena Carbone

Department of Chemical Science and Technologies, University of Rome Tor Vergata, Via della Ricerca Scientifica 1, 00133 Roma, Italy; carbone@uniroma2.it; Tel.: +39-06-7259-4470

Abstract: Personal, portable, and wearable electronics have become items of extensive use in daily life. Their fabrication requires flexible electronic components with high storage capability or with continuous power supplies (such as solar cells). In addition, formerly rigid tools such as electrochromic windows find new utilizations if they are fabricated with flexible characteristics. Flexibility and performances are determined by the material composition and fabrication procedures. In this regard, low-cost, easy-to-handle materials and processes are an asset in the overall production processes and items fruition. In the present mini-review, the most recent approaches are described in the production of flexible electronic devices based on NiO as low-cost material enhancing the overall performances. In particular, flexible NiO-based all-solid-state supercapacitors, electrodes electrochromic devices, temperature devices, and ReRAM are discussed, thus showing the potential of NiO as material for future developments in opto-electronic devices.

Keywords: NiO; flexible devices; synthesis; supercapacitors; electrodes; solar cells; electrochromic devices; temperature devices; ReRAM

check for updates

Citation: Carbone, M. NiO-Based Electronic Flexible Devices. *Appl. Sci.* **2022**, *12*, 2839. https://doi.org/10.3390/app12062839

Academic Editor: Andrea Li Bassi

Received: 2 January 2022
Accepted: 7 March 2022
Published: 10 March 2022

Publisher's Note: MDPI stays neutral with regard to jurisdictional claims in published maps and institutional affiliations.

Copyright: © 2022 by the author. Licensee MDPI, Basel, Switzerland. This article is an open access article distributed under the terms and conditions of the Creative Commons Attribution (CC BY) license (https://creativecommons.org/licenses/by/4.0/).

1. Introduction

Personal, portable and wearable electronics have become widely used in everyday life. Smart watches, smart glasses, fitness trackers, Bluetooth headsets are daily-life objects, which require the application of flexible electronic components. Flexible electronic technology offers a wide-variety of applications in cutting-edge areas such as biosensors [1–6], E-skin in robotics and prostheses [7], epidermal electronics [8], and biomedical instruments [9–12]. Furthermore, tactile sensors, can be built with signal processing technologies used to interpret the measured information from tactile sensors and/or sensors for other sensory modalities [13]. In addition, tools which are usually rigid, such as electrochromic devices, may also have wider applications if they are fabricated with flexible characteristics [14]. The assembling of these devices largely depends on the availability of flexible powering units such as batteries [15–19] solar cells [20], electrodes [21,22], transistors [23–27], display devices [28] conformable RFID (radio frequency identification) tags [29], and resistive random-access memories [30]. Traditional electronics are largely based on the integrated circuits mostly fabricated in rigid and planar semiconductor wafers, which fueled extensive research in associated phenomena on silicon surfaces [31–41]. However, they have limited applications in manufacturing flexible electronic devices due to the intrinsic rigidity of silicon wafers and the complex fabricating processes of its microstructure. Flexible materials, on the other hand, allow for large mechanical deformation, such as bending, twisting, stretching, and folding, which may fit irregular, soft, or moving objects such as human skin and wrinkled clothes [42,43]. Therefore, new materials have started being fabricated which are based on silicon nanoparticles integrated in elastomers [44], along with advanced materials and new architecture designs [45]. Simultaneously, supercapacitors with higher power density, faster recharge capability, safer operation, and longer cycle performance have become in demand to guarantee the devices operations with additional flexibility requirements. Materials such as graphene have emerged as a promising solution for building efficient, flexible electrochemical devices due to its unique electronic properties

and high optical transmittance [46–49]. However, high sheet resistance, low work function of pristine material [49], poor mechanical properties in presence of defects [50], and high strain limits curtail the actual graphene applications [51].

Combining flexibility requirements and enhanced performances may be achieved by integrating nanomaterials with the desired properties with suited flexible substrates resistant to deformations, mechanical stress, and of long duration.

Transition metal oxides and particularly NiO have the advantage of high storage capacitance [52], optical and electrical properties [53], transport properties on surfaces [54] as well as in perovskite solar cells [55]. Their nanoparticles synthesis may be achieved in several, environmentally friendly ways [56–63], with several shapes, arrangements, and super-structures [64]. Depending on the specific size and morphological characteristics, they can be employed in the construction of several types of devices for different purposes, which include chemosensing [65–68], supercapacitive devices [69–71], solar cells [72,73], and resistive memories [74–76].

Integrated NiO-based flexible materials can be achieved in several ways. NiO nanoparticles or thin films can be deposited on flexible materials such as PET (polyethylene terephthalate) or PEN (polyethylene naphthalate) substrates; NiO nanoparticles can be embedded in the flexible materials in the preparation phase, and NiO leagues can be de-alloyed [77] with a specific procedure that ensures ultimate pliability.

In the present mini-review, an overview of NiO synthetic methods and properties are reported as well as recent progresses in the fabrication and performances of NiO-based flexible devices. In particular, the latest constructions will be presented of NiO-flexible supercapacitors, electrodes, electrochromic devices, solar cells, temperature sensor devices, and resistive random-access memory.

2. Synthesis and Properties of NiO Nanoparticles and Thin Films

The NiO synthetic procedures largely condition its properties and make it suitable for different applications. Solvothermal (including sol-gel) and hydrothermal syntheses are among the most largely used methods, since they usually provide a facile way to tune size and shape of the NiO particles. Several parameters can be varied in both cases, such as type of Ni salt, type of base, temperature, solvent, and possible employment of a template. The employment of an autoclave also influences the course of the reaction due to the vapor pressure in a sealed vessel. Finally, the calcination phase, which typically follows, also plays a role, since it can shape the material depending on the temperature ramp and final temperature.

In addition, the phytogenic synthesis has become an interesting variant of the sol-gel method, where leaf extracts of plants such as *G. Sylvestre* [78] or *Ageratum conyzoides* L. [79] are used to form a gel which is to be removed during the calcination phase. NiO thin films can be achieved through several techniques: RF sputtering, electron beam evaporation, DC magnetron sputtering, anodic and cathodic electrodeposition, chemical vapor deposition, and nanoparticles electrospray [80]. A sketch of common synthetic pathways of NiO is reported in Figure 1, along with two examples of NiO thin film synthesis.

Finally, the dealloying technique has been successfully employed for achieving all-solid flexible materials, starting from various metals and metal oxides as an implementation of the achievement of flexible porous gold by the removal of silver from a gold-silver alloy with nitric acid [81].

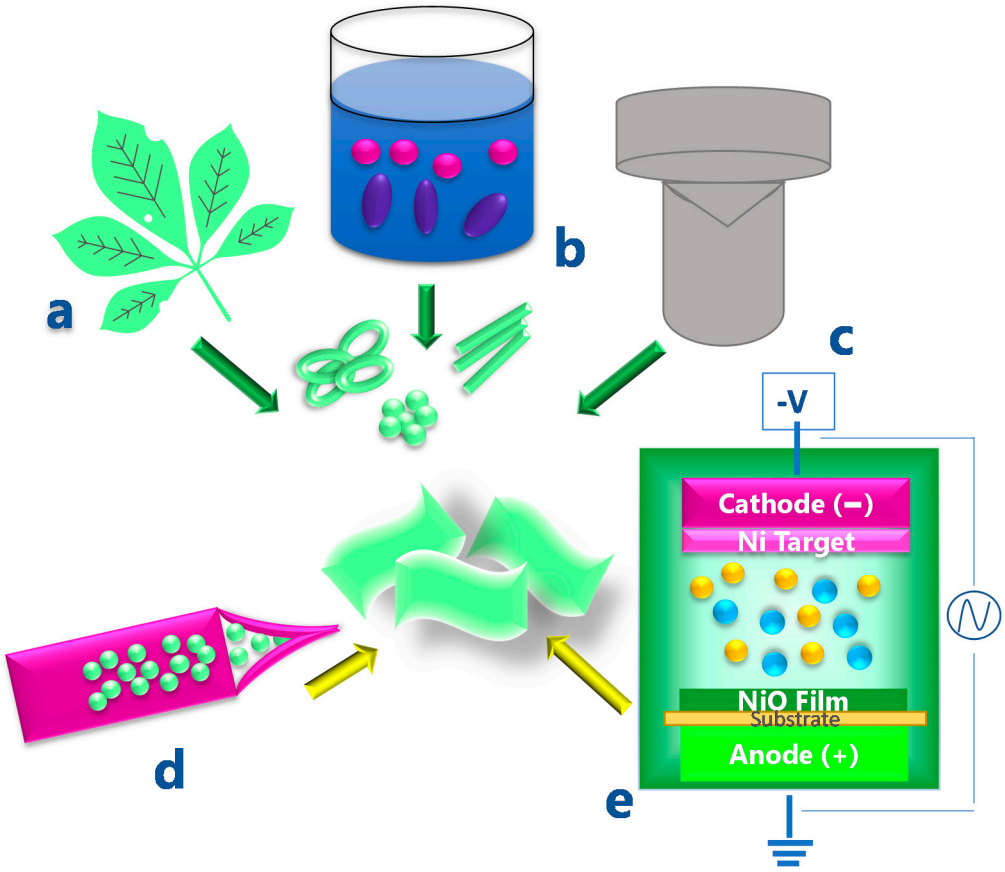

Figure 1. Sketch of the most common preparation methods of NiO nanoparticles and thin films: (**a**) phytosynthesis, (**b**) precipitation; (**c**) hydrothermal synthesis, (**d**) electrospray of nanoparticles to achieve thin film, (**e**) an example of RF sputtering technique for thin film synthesis. The blue and orange balls represent Ar and O_2 gases.

The type of conditions employed in the synthesis reflect onto the NiO properties. There are several examples of tuning the NiO features via the employment, for instance, of different types of bases which may influence the precursors structural parameters, such as the planar distances. The NiO morphology and the ensuing capacitance can be influenced by the calcination procedure [52,64,82]. The size of NiO nanoparticles is directly correlated to the band gap and can be estimated through the Brus relationship for spherical shapes [83]. Similarly, size and shape of the nanoparticles impact the NiO capacitance which is among the mostly exploited properties. Other relevant properties useful for building devices are the resistance variation with the temperature (Seebeck effect), the refractive index variation as a function of light wavelength, the hole mobility, and the resistance variation upon voltage application, which can be used for temperature devices, electrochromic devices, solar cells, and ReRAM, respectively.

The employment of NiO, either as nanoparticles or as thin layers in the actual construction of the various devices requires the embedding of NiO into matrices or the deposition on supports and ensuing incorporation in the device, with associated issues of integration feasibility and configuration design. The interaction NiO-matrix or NiO-support may influence the NiO properties through synergistic effects. Furthermore, the flexibility requirement may introduce the deterioration upon deformation, thus affecting the overall properties of the devices.

In Table 1, a few examples of capacitance dependency of NiO from morphologies as well as matrix and coating interactions are reported.

Table 1. Capacitance of NiO with various morphologies and composites.

NiO Morphology	Capacitance	Reference
Nanoparticles	423 F/g at 0.5 mA/cm^2	[84]
Nanoparticles	1012 mF/cm^2 at 1 mA/cm^2	[85]
Nanowires	670 F/g at 1 A/g	[86]
Nanoplates array	1124 F/g at 2 A/g	[87]
Microspheres	1482 F/g at 0.5 A/g	[88]
NiO Composites		
NiO@CeO_2 (5 wt%) Flower-like microspheres	2155.6 F/g at 1 A/g	[89]
NiO@CNT Particles	2480 F/g at 0.5 A/g	[90]
NiO-GNS/PANI	1409 F/g	[91]
NiO/GNS	1050 F/g	[92]
M-NiO-G//AC	154.0 F/g	[93]

The employment of NiO on a large scale needs to be offset against major drawbacks such as allergenicity and toxicity. In contact with the skin, NiO can cause allergic reactions [94] which is a problem for wearable devices exposing NiO on the external layer. Furthermore, it is especially harmful when inhaled [95], since it can induce an increased risk of lung cancer, as observed in epidemiological studies on rats [96]. In addition, the pouring out of NiO in waters and its bio-accumulation can represent an environmental hazard [97].

3. NiO-Based Flexible Devices

The usage of flexible, personal, portable, and wearable electronics and devices is subjected to the availability of similarly flexible storage apparatuses for power supply. Therefore, the first part of the mini-review is dedicated to the state-of-the-art NiO-based supercapacitors and electrodes (Section 3.1). Recently developed NiO-based flexible devices will be described in the following Sections 3.2–3.5.

3.1. Supercapacitors and Electrodes

Good flexibility as well as good electrochemical performances are achieved with NiO based cable-like all-solid-state flexible supercapacitor (CAF) [98]. In a recent report, a highly flexible electrode was constructed by achieving a sandwich of an interlayer of metallic glass (MG) and two outer layers of nanoporous nickel coated with nickel oxide/hydroxide (np-NiOxHy@Ni). The assembling of the sandwich was achieved in several steps, schematically reported in Figure 2. Metallic glass ribbons were obtained by arc-melting of pure metals (99.99 wt.%) under argon to yield the master alloy of $Ni_{40}Zr_{20}Ti_{40}$, followed by rapid quenching of the re-melted alloys onto a spinning copper roller [99,100] (Figure 2a). The outer layers were generated by immersing the as-spun ribbons in 0.05 M HF solutions for 4 h at 298 K to synthesize sandwich-like flexible np-NiOxHy@Ni/MG/np-NiOxHy@Ni composite electrodes (Figure 2b). Cable-like all-solid-state flexible supercapacitors (CAFSs) were prepared by soaking the nanoribbons in a gel obtained by heating an aqueous solution of PVA/KOH (Figure 2c). Then, two ribbons were twined on a rubber rod in the opposite direction and coated with gel electrolyte (Figure 2d). Finally, the CAFSs were prepared by wrapping with a thin cling film. Electrochemical measurements indicate that the electrode is essentially a battery-type material, also exhibiting pseudocapacitive behavior with a capacitance of 778 F cm^{-3} at 1 A cm^{-3} in KOH solutions and a retention of 80.3% when the current density increases by 128-fold, as well as a cycle stability of 100% capacitance retention after 8000 cycles.

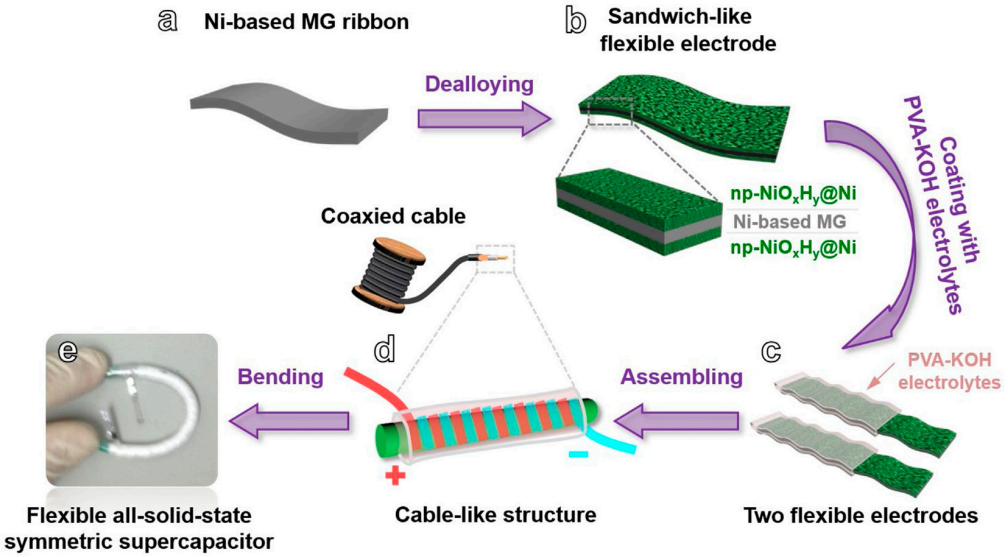

Figure 2. Scheme of the synthesis of sandwich-structured NiO-based flexible electrode and subsequently assembling of CAFS device (Reproduced from [98]. Copyright 2020, Elsevier: (**a**) Ni-based MG ribbon, (**b**) sandwich-like flexible electrode, (**c**) flexible electrodes after coating with PVA-KOH electrolytes, (**d**) flexible cable-like structure. (**e**) flexible all-solid-state symmetric supercapacitor.

The flexibility of the CAFSs was tested by performing cyclic voltammetry (CV) measurements with electrodes subjected to bending or twisting. The capacitance slightly increases by bending a 4 cm long electrode, until the distance between the extremes reaches 2 cm (nearly a U shape). With a further decrease of the distance, the capacitance slightly reduced. A capacitance retention of 96.4% could be obtained when the electrode was twisted into a shape of an "8". In addition, a capacitance retention of 92.4% was obtained after 1500 bending cycles.

Dealloying was also used for preparing a flexible $Co(OH)_2/NiO_xH_y$@Ni hybrid [101] with interwoven $Co(OH)_2$ nanopetals electrochemically deposited on the skeleton surface of np-NiO_xH_y electrodes. This was achieved by electrodeposition, using a three electrode cell immersed in a $Co(NO_3)_2 \cdot 6H_2O$ aqueous solution, where np-NiO_xH_y@Ni substrate acts as working electrode, a platinum plate is used as counter electrode and Ag/AgCl as reference electrode. Owing to the hierarchical porous structure and synergetic effect of $Co(OH)_2$ and NiO_xH_y electroactive materials, the $Co(OH)_2$/np-NiOxHy@Ni hybrid electrode delivered a voltage window of −0.1~0.6 V and a specific capacitance of 1421.1 F cm^{-3} at 0.5 A cm^{-3}, higher than the single transition-metal electrodes. Mounted on a watch, the supercapacitor could guarantee 45 min autonomy while being subjected to different deformations.

NiO-Plastisol Electrodes

Cheap, practical, flexible free standing electrodes were achieved by mixing synthetic graphite, with plasticizer agents (i.e., high molecular weight polyvinylchloride powder (PVC), bis(2-ethylhexyl)adipate (BEA) and THF [102]), followed by stirring, sonication, and solvent evaporation at room temperature overnight. NiO nanoparticles could be incorporated into the free-standing electrode by mixing them to the slurry, prior to the evaporation phase [103]. The resulting electrodes displayed a quite homogenous distribution of nanoparticles. Furthermore, NiO of different shapes and morphologies and at variable concentrations could be included.

In Figure 3A through c, the flexible NiO-decorated free standing electrode is shown. It can be cut with scissors (Figure 3A) in any kind of shape and size (Figure 3B), the original dimension being solely dependent on the size and shape of the glass tray hosting the slurry during the evaporation phase. Different morphologies of NiO were achieved by varying the synthesis condition, in particular the precipitating agent and the calcination

temperature. More in detail, triethylamine, NaOH and urea reacted with $Ni(NO_3)_2$ to yield $Ni(OH)_2$, converted into NiO by calcination at either 400 °C or 600 °C. The corresponding samples were labelled A (triethylamine), S (NaOH) or U (urea), followed by a 4 (400 °C) or 6 (600 °C). Overall, A4, A6, S6 and U6 NiO-decorated plastic electrodes were implemented for non-enzymatic amperometric detection of H_2O_2 in milk. The A4-NiO/plastisol displays the highest current density of all probed electrodes in response to H_2O_2 detection. This also corresponded to the best NiO dispersion within the plastisol matrix, though still retaining its original flower shape, as it can be appreciated at the backside of the electrode (Figure 3C—A4). A selection of SEM images of the flexible NiO-doped electrodes (front- and backside) is reported in Figure 3C. When probed on commercial milk, the A4-NiO/plastisol electrode reached a LOD of 5 µM and a linearity range up to 4 mM.

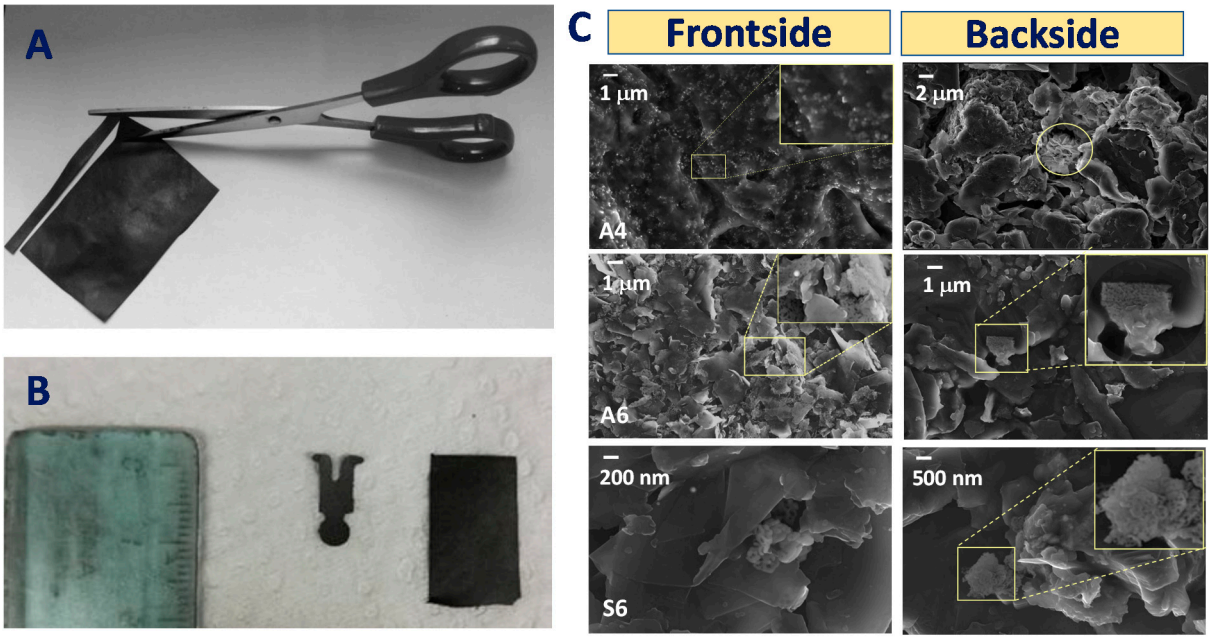

Figure 3. Flexible NiO-based plastisol free-standing electrode. (**A**) Photograph of the flexible, croppable electrode. (**B**) An example of a customized shape of NiO-plastisol sheet and an indication of the dimensions. (**C**) SEM images of front and back sides the NiO-plastisol electrodes obtained with NiO of different morphologies (Reproduced from [103], with modifications).

3.2. Resistive Random Access Memory

Resistive random access memory (ReRAM) is considered the most promising among the flexible non-volatile memories (NVMs) due to its simple metal-insulator-metal (MIM) structure, high switching speed, low power consumption, low operating temperature, and high packaging density. Flexible ReRAM is essential in smart wearable electronics and all-in-one fully flexible electronic system, since flexible memory is a fundamental component for data processing, storage, and communication with external devices.

NiO based ReRAM has the advantage of stable switching properties at specific conditions, lower operation set/reset current and forming voltage in comparison to other metal oxides. A flexible NiO ReRAM device with good operation characteristics was achieved, based on a solution process using NiO nanocrystals (NC), on flexible PET substrate [104]. The construction of the ReRAM devices consisted in the deposition of a 100-nm-thick platinum (Pt) and a 20 nm-thick titanium (Ti) adhesion layer on a polymer substrate using an e-beam evaporator. A dispersion of NiO-NCs and isopropyl-alcohol (IPA) was dropped on the flexible PET substrate, and the NiO-NC solution pressed by a poly—dimethylsiloxane (PDMS) mold while heating at 80 °C. The excess of coated NiO-NC solution leaking out, as well as the residual layer, were removed and the PDMS mold was demolded from the substrate, leaving a NiO nanopillar array fabricated on the substrate without NC residue.

The electric signal and bias voltage were probed by a Pt/Ti-coated Si AFM tip contacted on nanoscale ReRAM devices, by applying a voltage on the top electrode, while the bottom electrode was grounded, and the resistance values of the NiO ReRAM were read at 0.01 V. The flexible NiO ReRAM device exhibited unipolar resistive switching behaviors corresponding to those of an evaporated NiO thin film. The switching behavior was initiated at 11 V with 0.04 V and 1 μA current compliance by a conductive filament forming operation. For the reset switching of the NiO flexible ReRAM, the voltage was swept from 0 V to 5 V with 0.02 V. The resistance of the NiO ReRAM device changed from 102 Ω to 107 Ω at 2.4 V for reset switching, and the set switching was operated in reverse at 3.4 V. The flexibility of the device is demonstrated by a nearly 180° bending as shown in Figure 4, along with the SEM imaging indicating the NiO-NC patterning of the PET substrate.

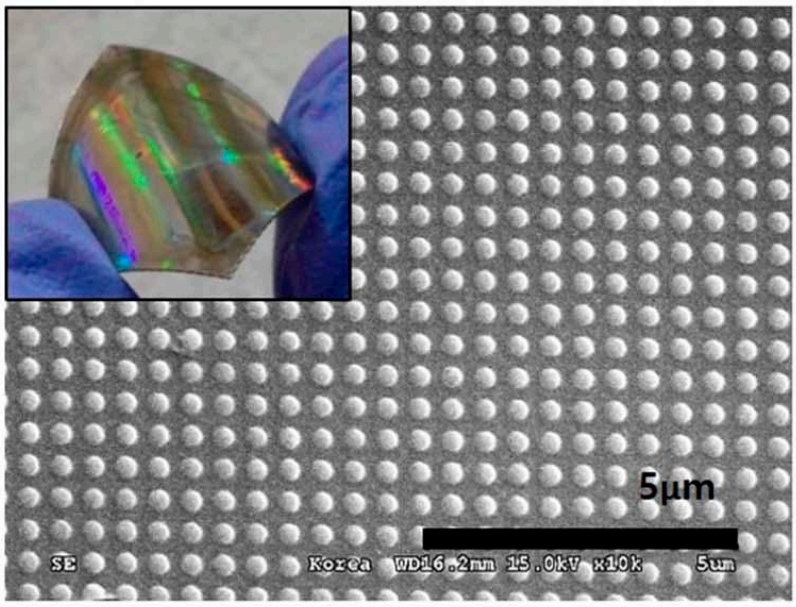

Figure 4. SEM image of a flexible NiO ReRAM device on flexible PET substrate. (Reproduced from [104], Copyright 2021, Elsevier).

3.3. Electrochromic Devices

Electrochromism is the reversible color change of an electrochromic device (ECD) under an applied voltage. NiO is among the transition metals reportedly displaying the best electrochromic properties as anodic material, though associated drawbacks may be a low optical modulation, short-term stability, and slow switching time. These pitfalls can be overcome by modulating the NiO properties through synthetic strategies. A facile solid-state strategy for the preparation of NiO particles [105] foresaw a solid-state calcination of nickel acetate dihydrate at 600–900 °C, followed by NiO ink preparation by mixture with solvents (chlorobenzene, a 2:1 isopropanol-water mixture, or chloroform) sonication and sedimentation. According to this procedure, the ink was subsequently spin-coated on cleaned ITO glass and flexible Ag/PET substrates. The latter, in particular, was achieved by subsequently coating AgNanoWire (AgNW), poly(3,4-ethylenedioxythiophene) polystyrene sulfonate (PEDOT: PSS, 5 wt% in ethanol) and NiO ink onto the PET substrate. Analogous films were synthesized using WO_3 particles. Devices were built using a NiO film as working electrode and PEDOT:PSS/AgNW/PET or WO_3—coated PEDOT: PSS/AgNW/PET as the counter electrodes. The NiO and NiO/WO_3 ECDs on ITO substrate exhibited a transmittance variation of ΔT = ~84% at 700 nm between −3.0 and 0 V. The flexible NiO/WO_3 device achieved ΔT = ~38% at 700 nm between 2.0 V–0 V for, indicating a potentially use in smart windows and optical devices.

The properties of NiO can be modified by doping, for instance with tungsten to achieve $Ni_{1-x}W_xO$, which is suitable as anode in electrochromic devices. In this framework, the

employment of doped oxides required a preliminary optimization procedure to determine the most suited $Ni_{1-x}W_xO$ composition. To this purpose, the electrochromic properties of $Ni_{1-x}W_xO$ were evaluated by varying the W atomic percentage in a range between 0 and 20% and performing measurements in lithium perchlorate and propylene carbonate. Enhanced cycle stability with moderate optical modulation was obtained for a $Ni_{1-x}W_x$ oxide film with at x = 0.024 [106]. Flexible electrochromic devices employing $Ni_{1-x}W_xO$ were fabricated on a PET substrate with monolayered graphene as a platform, thus creating stacked layers of PET, ITO, graphene, WO_3 and $Ni_{1-x}W_xO$ thin films. In particular, the flexible electrochromic device was achieved by growing a single layered graphene on Cu foil (99.8%) by rapid thermal chemical vapor deposition (RTCVD). A procedure of DC magnetron sputtering at RT and subsequent post-annealing process at 250 °C was used to fabricate highly crystalline ITO (c-ITO) on graphene/Cu foil with a thickness of 60 nm, which was afterwards continuously transferred onto a PET substrate. The c-ITO/graphene/PET electrode showed a sheet resistance of ~45 Ω/sq and a transmittance of ~92% at a wavelength of 550 nm. The flexible EC devices were fabricated by laminating the WO_3 film and optimizing the $Ni_{0.976}W_{0.024}O$ film deposited on the c-ITO/graphene/PET substrate, using Li-based polymeric solid-state electrolyte. The flexible EC device showed stable cycling performances, maintaining an optical modulation of $\Delta T \approx 40\%$. In addition, the flexible EC device showed stable optical modulation, with a ~2% reduction after 1000 cycles.

3.4. Temperature Devices

Flexible, resistive temperature detectors (RTDs) allow temperature measurements in wearable devices. In addition, the coupling to RFID converts them into wireless sensors which can be used for checking the body temperature, short-life span food and medications. The main requirements of such devices are a high and linear temperature coefficient of resistance (TCR), high resistance to bending and deformation and simplicity of design and measurements. A Ni/NiO based resistive temperature detector (RTDs) was proposed with such characteristics, based on the layered deposition on a PET fiber [107]. The device was fabricated by depositing a Ni/NiO bilayer on a bare cylindrical PET fiber pre-treated by sonication in acetone for 10 min, followed by sonication in methanol for 10 more min, washing and drying. NiO and Ni were deposited on the rotating PET fiber substrate by Radio Frequency magnetron sputtering, ensuring simultaneous argon and oxygen flow for NiO deposition and argon flow for the Ni thin film second coat. Resistance variation measurements with the temperature indicated that the device had a TCR of 3.8×10^{-3} °C^{-1} and a linearity of 0.9852. The bending process simulated movements through daily activities. After 16,000 bends the TCR of the device was 1.0×10^{-4} °C^{-1} with a linearity of 0.9065. Additional tests were performed washing with tap water and laundry detergent and exposing to acidic and basic environment. The electrical properties including resistance, TCR and linearity of slope remained unaffected when subjected to the different conditions. Moreover, the device maintained about 75% of the original TCR after being exposed to an acidic medium.

3.5. Solar Cells

Flexible inverted perovskite solar cells (PSCs) are achieved using a glass/ITO substrate as conductive transparent layer, and NiO_x as an effective hole-transport material. Several variants were probed, with the purpose of achieving a high-power conversion efficiency (PCE) while keeping flexibility. Compared to normal PSCs, inverted flexible PSCs are light weighted, compatible with different surfaces, and portable, thus meeting the demands of the electronics industry [108,109]. Their further development, however, depends on the quality and characteristics of the hole transport layer (HTL). In this regard, NiO_x is a promising candidate, owing to its low-temperature processing and good electron-blocking ability. In a relatively simple construction [110] NiO_x nanofilms were deposited on ITO-PEN by spin coating from a high quality NiO_x nanoparticle solution pre-synthesized by

precipitation. Perovskite was deposited on top of the NiO_x layer by spin coating, after achieving a precursor by reacting PbI_2 and CH_3NH_3I in a mixture of DMSO and DMF, dripping chlorobenzene during spinning and baking at 100 °C. A thin layer of phenyl-C61-butyric acid methylester and a layer of Ag 150 nm thick completed the inverted planar heterojunction solar cells. The as-prepared NiO_x films had excellent hole extraction and electron blocking property, thus providing a good hole contact for perovskite solar cells. A maximum PCE of 16.47% (steady state PCE of 16.21%) was achieved for the NiO_x-based perovskite solar cell on the ITO-PEN glass substrate.

In order to improve the band structure alignment between low-temperature-processed NiO_x and the perovskite layer, amino-functionalized graphene quantum dots (AGQDs) were included in the NiO_x film as a dual-role additive. In addition, the AGQDs can provide abundant N atoms at the modified NiO_x layer surface to enhance the crystallization of the perovskite film by a Lewis base-acid interaction. On the other hand, the AGQDs can optimize the band structure alignment between the NiO_x and perovskite layers, facilitating hole extraction at the NiO_x/perovskite interface [111]. The overall building up of AGQDs-aided NiO/peroskite flexible solar cells requires the separate synthesis of AGQDs, NiO_x ink and subsequent assembling on PEN/ITO substrate after etching. More in detail, AGQDs were achieved by RT reaction of graphene sheets with ammonia, followed by autoclave treatment at 150 °C for 5 h and dialysis of the cooled solution. NiO_x was prepared by reaction of $Ni(NO_3)_2$ with NaOH at pH 10, drying of the precipitate at 80 °C and calcination at 275 °C for 2 h. The pristine NiO_x ink was prepared by dispersing 20 mg of NiO_x powder in 1 mL of deionized water. AGQD-doped NiO_x inks were obtained by directly mixing AGQD aqueous solutions with the pristine NiO_x ink. The pristine and AGQD-doped NiO_x inks were spin-coated on the flexible substrates, heated at 120 °C for 15 min and transferred to a N_2-filled glovebox to prepare the perovskite films. The resulting inverted flexible PSC was subjected to automatic bending and exhibited an efficiency of 18.10%, good air stability, retention of 88% of its initial efficiency after continuously bending 1000 times and a retention of 64% of the initial efficiency after 30 days.

4. Electronic Flexible Devices Based on Other Oxides

Flexible supercapacitors are typically achieved by embedding an active material in a flexible support, usually a carbon-based material, including active carbon, graphene, carbon nanotubes, aerogel and hydrogels [112,113], unless techniques such as the dealloying can be applied. More recently, the use of paper supports was implemented for one-time only devices [114]. Several transition metal oxides (TMO), alone and in association with conducting polymers, were probed on flexible supports to achieve supercapacitors. ZnO/carbon nanofibers attained by electrospinning showed a specific capacitance > 100 Fg^{-1} and retention capability of 93.90% after 2000 continuous charge/discharge cycles [115]. A porous carbonized cotton/ZnO/CuS composite electrode showed a specific capacitance of 1830 mF cm^{-2} at 2 mA cm^{-2} and 74% retention with the current density increasing from 2 to 10 mA cm^{-2} and a loss of 14.8% of the initial capacitance after 5000 cycles [116]. An Fe_2O_3/Graphene aerogel hybrid electrode was used to build a highly flexible all-solid-state symmetric supercapacitor device, which could be bent by several angles providing a high specific capacitance, i.e., 440 Fg^{-1} and 90% capacitance retainment over 2200 cycles [117]. Confined anatase TiO_2 nanoparticles were achieved in conductive activated carbon interconnected nanopores. The assembled cells with porous carbon cathodes displayed a specific capacity of ≈140 mAh g^{-1} at slow charge and ≈60 mAh g^{-1} at a 3.5 s fast charge [118]. Compared to the most recent NiO-based supercapacitors or electrodes, these systems show either a slightly lower performance or lower retention of properties upon deformation.

Flexible temperature devices have been fabricated using many different types of active materials on flexible supports deposited with different techniques. The most common active materials in temperature sensors are Pt and Au. They were deposited on a polyimide film after a peeling process, for monitoring the temperature in the range 20–120 °C and displayed a TCR value of 0.0032 $°C^{-1}$ [119]. Cr and Au thin layers were sputtered on

pre-stretched PDMS to minimize the tensile strain [120] and create a reversible bendable and stretchable flexible temperature device.

Ag lines on polyimide were evenly distributed by inkjet printing and constituted a bendable and flexible sensor for measuring body surface temperatures in the 20–60 °C range, with an average sensitivity of 2.23 × 103 $°C^{-1}$ and less than 5% hysteresis [121].

ReRAMs are typically constituted of a top and a bottom electrode interlayered either by a semiconductor or by an insulating layer. The ReRAM performances are usually related to the interlayer, though the choice of the electrodes also plays a role. As for the interlayers, they are usually categorized into two groups, namely organic and inorganic. The organic interlayers include, among the others, silk protein/fibroin, nanocellulose and albumen [122–124]. These devices, however, tend to be rather humidity sensitive and not very stable in long terms operations. Metal oxides are typical inorganic interlayers, and a vast amount of electrode interlayer combinations was probed. Bipolar ReRAM devices were achieved, for instance, based on Pd/HfO_x-Ag NPs/TiN [125], or Ag/MnO-Ta_2O_5/Pt [126]. The former operates at a set voltage of 2.2 V and reset voltage at −2.2 V, the latter at a set voltage of 0.8 V and reset voltage at −1.1 V. Unipolar ReRAM are more difficult to achieve. Some examples are provided by Al/HfO_x/Al (set voltage 1.8 V, reset voltage 0.8 V) [127] and Pt/ZnO/Pt (set voltage 1.1–2.3 V, reset voltage 0.4–1 V) [128]. The issue of flexibility of ReRAM, however, is difficult to tackle, also due to the necessity of incorporating the electrodes in the device. This was achieved, so far in a Ni/Sm_2O_3/ITO device, which can operate at very low power (set: 0.25 V, 100 µA and vice versa, reset: 0.20 V, 49 µA) [129] or more recently with Ag/Au-chitosan/Au (bipolar, set voltage of 2.5 V) [130], which is biocompatible, but does not overcome the costs and fabrication related issues.

The development of flexible electrochromic devices is connected to the possibility of achieving a uniform layer of color changing material on a flexible substrate, capable of retaining the properties under stress and over time. Besides NiO based materials, recent developments were achieved using 2D TiO_2/MXene heterostructures on PET [131]. More in detail, TiO_2/$Ti_3C_2T_x$ heterostructures were employed where the $Ti_3C_2T_x$ film serves as the transparent conductive electrode, and the TiO_2 film serves as the EC layer in EC devices. The heterostructure was prepared through an aerogel formation, dispersion in IPA and ensuing deposition on the substrate. At 550 nm, the transmittance variation reaches its maximum at around 60%, and it is largely retained upon 1000 EC cycles (92%), thus offering a practical alternative to NiO based EC devices.

A different issue is the employment NiO in perovskite flexible solar cells since it is a rather standard layer for the hole transport and difficult to replace.

On average, NiO-based devices have the advantage of a low cost, especially when compared to Au/Pt based thermometers, or to HfO_x ReRAM, as well as a better retention of properties upon deformation. In addition, NiO-based devices have more stable switching properties.

5. Future Perspectives and Conclusions

Flexible devices are largely in demand due to the rising tendency for good fitting, comfortable, easy-to-use tools and materials, which can feed the creativity of fashion designs. In addition, practicality, improved operativity and portability of smart devices for well-being aid the monitoring of vital parameters for personalized drug-delivery based on actual needs (all-in-all helping to maintain a healthy lifestyle).

To a larger scale, modern, eco-sustainable architecture requires the use of materials which are adaptable, versatile, and energetically self-standing. The future development of flexible devices is very much connected to the development of integrated flexible components with homogenous characteristics of durability which ensure the proper functioning of the devices, a low-cost production and can be easily recharged if necessary. In this framework, some recently developed flexible tools were presented based on NiO as low-cost active material, which can give rise to improved flexible technology for the pursue of personalized items and tailored devices.

NiO-based flexible supercapacitors may b achieved by the de-alloying, a technique that allows the fabrication of all-solid-state devices with associated advantages over the employment of liquid electrolytes (which may be affected by leakage and transport issues). These devices are characterized by a capacitance comparable to analoguesbased on 2D materials and higher resilience to repeated bending and deformation cycles [132]. The embedding of NiO is fundamental to enhance the electrochemical response of the plastisol towards specific targets such as H_2O_2. Overall, the hybrid NiO-plastisol material has performances, to some extent, comparable to other non-flexible electrodes (see Table 3 in Ref. [103]), with the additional advantage of its flexibility.

The examined NiO flexible temperature device showed a large resistance to harsh basic and acidic conditions (as compared, for instance, to graphene ribbons-based devices) and less sensitivity to the oxidative conditions in the synthesis procedure (which affects the reproducibility of the production of graphene derivatives-based devices) [133].

Flexible resistive random-access memory devices are usually achieved by employing a supple support topped by an active layer. Several options were suggested as active material, such as black phosphorous [134] or graphene oxide [135]. However, in both cases, limitations arise from the difficulty of handling the material in safe conditions or to achieve stability and/or stable performances (in addition to the employment of expensive connection Au layers) [135].

NiO-based electrochromic devices have better optical contrast, shorter coloring and bleaching times as compared to other inorganic analogues such as Ag-nanowire based ones [136], and cheaper manufacturing, due to lower cost of production materials.

For solar cells the use of NiO is, in a way, essential, since it is routinely used as HTL, the real challenge being the insertion of the NiO component in flexible structures while keeping or improving the conversion efficiency.

However, the manufacturing techniques may strongly impact the performances of the electronic devices. The retention of properties and consequent scalability of the processes is usually more favorable for flexible materials prepared by physical deposition methods. However, these are lengthy and costly procedures. Therefore, the development of solution-processable materials is preferred for device assembling. In this regard, the molding as well as the ink deposition and printing techniques are the most promising for the fabrication of devices. Furthermore, a correct assessment of the performances upon stress would require several deformation tests, including stretching and compression (besides bending), especially for the electronic materials destined to wearable devices. Therefore, a complete evaluation of performances under stress is advisable for the planning of a device.

In general, NiO provides the benefits of a low-cost material, which can be easily adapted to the specific needs through tailored synthetic pathways. The use of NiO may be of source of concern when included into devices which come in contact with the skin since it can induce allergic reactions. Furthermore, it can be considered a bio-hazard since it enhances the risks of lungs cancer. Therefore, sealing must be ensured of the NiO containing component to avoid leakage and ensuing adverse responses.

In summary, NiO-based flexible devices provide quite often a practical, efficient, resilient, and low-cost option to fulfill the increasing demand of flexible technology.

Funding: This research received no external funding.

Institutional Review Board Statement: Not Applicable.

Informed Consent Statement: Not Applicable.

Conflicts of Interest: The author declares no conflict of interest.

References

1. Mannsfeld, S.C.; Tee, B.C.; Stoltenberg, R.M.; Chen, C.V.; Barman, S.; Muir, B.V.O.; Sokolov, A.N.; Reese, C.; Bao, Z. Highly sensitive flexible pressure sensors with microstructured rubber dielectric layers. *Nat. Mater.* **2010**, *9*, 859. [CrossRef] [PubMed]
2. Yamada, T.; Hayamizu, Y.; Yamamoto, Y.; Yomogida, Y.; Izadi-Najafabadi, A.; Futaba, D.N.; Hata, K. A stretchable carbon nanotube strain sensor for human-motion detection. *Nat. Nanotechnol.* **2011**, *6*, 296. [CrossRef] [PubMed]

3. Yang, Y.; Gao, W. Wearable and flexible electronics for continuous molecular monitoring. *Chem. Soc. Rev.* **2019**, *48*, 1465–1491. [CrossRef] [PubMed]
4. Schwartz, G.; Tee, B.C.K.; Mei, J.; Appleton, A.L.; Kim, D.H.; Wang, H.; Bao, Z. Flexible polymer transistors with high pressure sensitivity for application in electronic skin and health monitoring. *Nat. Commun.* **2013**, *4*, 1859. [CrossRef] [PubMed]
5. Choong, C.L.; Shim, M.B.; Lee, B.S.; Jeon, S.; Ko, D.-S.; Kang, T.-H.; Bae, J.; Lee, S.-H.; Byun, K.-E.; Im, J.; et al. Highly stretchable resistive pressure sensors using a conductive elastomeric composite on a micropyramid array. *Adv. Mater.* **2014**, *26*, 3451. [CrossRef] [PubMed]
6. Trung, T.Q.; Lee, N.E. Flexible and stretchable physical sensor integrated platforms for wearable human-activity monitoring and personal healthcare. *Adv. Mater.* **2016**, *28*, 4338–4372. [CrossRef] [PubMed]
7. Zhu, H.; Wang, X.H.; Liang, J.; Lv, H.; Tong, H.; Ma, L.; Hu, Y.; Zhu, G.; Zhang, T.; Tie, Z.; et al. Versatile electronic skins for motion detection of joints enabled by aligned few-walled carbon nanotubes in flexible polymer composites. *Adv. Funct. Mater.* **2017**, *27*, 1606604. [CrossRef]
8. Kim, D.H.; Lu, N.; Ma, R.; Kim, Y.-S.; Kim, R.-H.; Wang, S.; Wu, J.; Won, S.M.; Tao, H.; Islam, A.; et al. Epidermal electronics. *Science* **2011**, *333*, 838. [CrossRef] [PubMed]
9. Kenry, J.C.Y.; Lim, C.T. Emerging flexible and wearable physical sensing platforms for healthcare and biomedical applications. *Microsyst. Nanoeng.* **2016**, *2*, 16043. [CrossRef] [PubMed]
10. Lacour, S.P.; Benmerah, S.; Tarte, E.; FitzGerald, J.; Serra, J.; McMahon, S.; Fawcett, J.; Graudejus, O.; Yu, Z.; Morrison, B. Flexible and stretchable micro-electrodes for in vitro and in vivo neural interfaces. *Med. Biolog. Eng. Comput.* **2010**, *48*, 945–954. [CrossRef] [PubMed]
11. Jeong, J.W.; Kim, M.K.; Cheng, H.; Yeo, W.-H.; Huang, X.; Liu, Y.; Zhang, Y.; Huang, Y.; Rogers, J.A. Capacitive epidermal electronics for electrically safe, long-term electrophysiological measurements. *Adv. Healthc. Mater.* **2014**, *3*, 642–648. [CrossRef] [PubMed]
12. Yang, Y.; Yang, X.; Zou, X.; Wu, S.; Wan, D.; Cao, A.; Liao, L.; Yuan, Q.; Duan, X. Ultrafine graphene nanomesh with large on/off ratio for high-performance flexible biosensors. *Adv. Funct. Mater.* **2017**, *27*, 1604096. [CrossRef]
13. Zou, L.; Ge, Z.C.; Wang, J.; Cretu, E.; Li, X. Novel Tactile Sensor Technology and Smart Tactile Sensing Systems: A Review. *Sensors* **2017**, *17*, 2653. [CrossRef] [PubMed]
14. Eh, A.L.-S.; Tan, A.W.M.; Cheng, X.; Magdassi, S.; Lee, P.S. Recent Advances in Flexible Electrochromic Devices: Prerequisites, Challenges, and Prospects. *Energy Technol.* **2018**, *6*, 33–45. [CrossRef]
15. Chen, Z.; To, J.W.F.; Wang, C.; Lu, Z.; Liu, N.; Chortos, A.; Pan, L.; Wei, F.; Cui, Y.; Bao, Z. A three-dimensionally interconnected carbon nanotube-conducting polymer hydrogel network for high-performance flexible battery electrodes. *Adv. Energy Mater.* **2014**, *4*, 1400207. [CrossRef]
16. Lin, H.; Weng, W.; Ren, J.; Qiu, L.; Zhang, Z.; Chen, P.; Chen, X.; Deng, J.; Wang, Y.; Peng, H. Twisted aligned carbon nanotube/silicon composite fiber anode for flexible wire-shaped lithium-ion battery. *Adv. Mater.* **2014**, *26*, 1217–1222. [CrossRef] [PubMed]
17. Gwon, H.; Hong, J.; Kim, H.; Seo, D.-H.; Jeon, S.; Kang, K. Recent progress on flexible lithium rechargeable batteries. *Energy Environm. Sci.* **2014**, *7*, 538–551. [CrossRef]
18. Chen, L.; Zhou, G.; Liu, Z.; Ma, X.; Chen, J.; Zhang, Z.; Ma, X.; Li, F.; Cheng, H.-M.; Ren, W. Scalable clean exfoliation of high-quality few-layer black phosphorus for a flexible lithium ion battery. *Adv. Mater.* **2016**, *28*, 510–517. [CrossRef] [PubMed]
19. Mo, R.; Rooney, D.; Sun, K.; Yang, H.Y. 3D nitrogen-doped graphene foam with encapsulated germanium/nitrogen-doped graphene yolk-she, ll nanoarchitecture for high-performance flexible Li ion battery. *Nat. Commun.* **2017**, *8*, 13949. [CrossRef] [PubMed]
20. Li, X.; Li, P.; Wu, Z.; Luo, D.; Yu, H.-Y.; Lu, Z.-H. Review and perspective of materials for flexible solar cells. *Mater. Rep. Energy* **2021**, *1*, 100001. [CrossRef]
21. Dong, S.; Xi, J.; Wu, Y.; Liu, H.; Fu, C.; Liu, H.; Xiao, F. High loading MnO_2 nanowires on graphene paper: Facile electrochemical synthesis and use as flexible electrode for tracking hydrogen peroxide secretion in live cells. *Anal. Chim. Acta* **2015**, *853*, 200–206. [CrossRef]
22. Nagaraju, G.; Raju, G.S.R.; Ko, Y.H.; Yu, J.S. Hierarchical Ni–Co layered double hydroxide nanosheets entrapped on conductive textile fibers: A cost-effective and flexible electrode for high-performance pseudocapacitors. *Nanoscale* **2016**, *8*, 812–825. [CrossRef]
23. Pu, J.; Yomogida, Y.; Liu, K.-K.; Li, L.-J.; Iwasa, Y.; Takenobu, T. Highly flexible MoS2 thin film transistors with ion gel dielectrics. *Nano Lett.* **2012**, *12*, 4013–4017. [CrossRef]
24. Lee, G.H.; Yu, Y.J.; Cui, X.; Petrone, N.; Lee, C.-H.; Choi, M.S.; Lee, D.-Y.; Lee, C.; Yoo, W.J.; Watanabe, K.; et al. Flexible and transparent MoS_2 field-effect transistors on hexagonal boron nitride-graphene heterostructures. *ACS Nano* **2013**, *7*, 7931–7936. [CrossRef]
25. Chortos, A.; Lim, J.; To, J.W.F.; Vosgueritchian, M.; Dusseault, T.J.; Kim, T.H.; Hwang, S.; Bao, Z. Highly stretchable transistors using a microcracked organic semiconductor. *Adv. Mater.* **2014**, *26*, 4253–4259. [CrossRef]
26. Park, S.; Shin, S.H.; Yogeesh, M.N.; Lee, A.L.; Rahimi, S.; Akinwande, D. Extremely high-frequency flexible graphene thin-film transistors. *IEEE Electron Device Lett.* **2016**, *37*, 512–515. [CrossRef]
27. Kim, Y.H.; Lee, E.Y.; Lee, H.H.; Seo, S. Characteristics of reduced graphene oxide quantum dots for a flexible memory thin film transistor. *ACS Appl. Mater. Interfaces* **2017**, *9*, 16375–16380. [CrossRef]

28. Liang, J.; Li, L.; Niu, X.; Pei, Q. Elastomeric polymer light-emitting devices and displays. *Nat. Photonics* **2013**, *7*, 817–824. [CrossRef]
29. Jung, M.; Kim, J.; Noh, J.; Lim, N.; Lim, C.; Lee, G.; Kim, J.; Kang, H.; Jung, K.; Leonard, A.D.; et al. All-printed and roll-to-roll-printable 13.56-MHz-operated 1-bit RF tag on plastic foils. *IEEE Trans. Electron Devices* **2010**, *57*, 571. [CrossRef]
30. Gupta, V.; Kapur, S.; Saurabh, S.; Grover, A. Resistive Random Access Memory: A Review of Device Challenges. *IETE Tech. Rev.* **2020**, *37*, 377–390. [CrossRef]
31. Casaletto, M.P.; Zanoni, R.; Carbone, M.; Piancastelli, M.N.; Aballe, L.; Weiss, K.; Horn, K. Ethylene adsorption on Si(100)2 × 1: A high-resolution photoemission study. *Phys. Rev. B* **2000**, *62*, 17128–17133. [CrossRef]
32. Kim, J.W.; Carbone, M.; Tallarida, J.H.; Dil, M.; Horn, K.; Casaletto, M.P.; Flammini, R.; Piancastelli, M.N. Adsorption of 2,3-butanediol on Si(100). *Surf. Sci.* **2004**, *559*, 179–185. [CrossRef]
33. Carbone, M.; Caminiti, R. Adsorption states and site conversions of phenylacetylene on Si(100)2 × 1 calculated by DFT. *J. Theor. Comput. Chem.* **2012**, *11*, 1089–1099. [CrossRef]
34. Carbone, M.; Piancastelli, M.N.; Zanoni, R.; Comtet, G.; Dujardin, G.; Hellner, L. Methanol adsorption on Si(111)-(7 × 7), investigated by core-line photoemission and mass spectrometry of photodesorbed ions. *Surf. Sci.* **1997**, *370*, L179–L184. [CrossRef]
35. Carbone, M.; Zanoni, R.; Piancastelli, M.N.; Comtet, G.; Hellner, L.; Mayne, A. Adsorption of ethylene on Si(111)7 × 7 by synchrotron radiation photoemission. *J. Electron Spectrosc.* **1995**, *76*, 271–276. [CrossRef]
36. Carbone, M.; Piancastelli, M.N.; Casaletto, M.P.; Zanoni, R.; Besnard-Ramage, M.J.; Comtet, G.; Dujardin, G.; Hellner, L. Phenol adsorption on Si (111)7 × 7 studied by synchrotron radiation photoemission and photodesorption. *Surf. Sci.* **1999**, *419*, 114–119. [CrossRef]
37. Flammini, R.; Cecchetti, D.; Tagliatesta, P.; Carbone, M. Multiple options for phenol on Si(111)7 × 7 revealed by high resolution photoemission. *Surf. Sci.* **2020**, *692*, 121510. [CrossRef]
38. Carbone, M.; Zanoni, R.; Piancastelli, M.N.; Comtet, G.; Dujardin, G.; Hellner, L. Synchrotron radiation photoemission and photostimulated desorption of deuterated methanol on Si(111)7 × 7 and Si(100)2 × 1. *Surf. Sci.* **1996**, *352–354*, 391–395. [CrossRef]
39. Carbone, M.; Piancastelli, M.N.; Paggel, J.J.; Weindel, C.; Horn, K. A high-resolution photoemission study of ethanol adsorption on Si(111)-(7 × 7). *Surf. Sci.* **1998**, *412–413*, 441–446. [CrossRef]
40. Carbone, M.; Caminiti, R. Fragmentation pathways of acetic acid upon adsorption on Si(100)2 × 1. *Surf. Sci.* **2008**, *602*, 852–858. [CrossRef]
41. Carbone, M.; Meloni, S.; Caminiti, R. Dissociative versus molecular adsorption of phenol on Si (100) 2 × 1: A first-principles calculation. *Phys. Rev. B* **2007**, *76*, 085332. [CrossRef]
42. Hammock, M.L.; Chortos, A.; Tee, B.C.K.; Tok, J.B.-H.; Bao, Z. 25th anniversary article: The evolution of electronic skin (e-skin): A brief history, design considerations, and recent progress. *Adv. Mater.* **2013**, *25*, 5997. [CrossRef] [PubMed]
43. Rogers, J.A.; Someya, T.; Huang, Y. Materials and mechanics for stretchable electronics. *Science* **2010**, *327*, 1603. [CrossRef] [PubMed]
44. Ying, M.; Bonifas, A.P.; Lu, N.; Su, Y.; Li, R.; Cheng, H.; Ameen, A.; Huang, Y.; Rogers, J.A. Silicon nanomembranes for fingertip electronics. *Nanotechnology* **2012**, *23*, 344004. [CrossRef] [PubMed]
45. Zou, M.; Ma, Y.; Yuan, X.; Hu, Y.; Liu, J.; Jin., Z. Flexible devices: From materials, architectures to applications. *J. Semicond.* **2018**, *39*, 011010. [CrossRef]
46. Valentini, F.; Roscioli, D.; Carbone, M.; Conte, V.; Floris, B.; Palleschi, G.; Flammini, R.; Bauer, E.M.; Nasillo, G.; Caponetti, E. Oxidized graphene in ionic liquids for assembling chemically modified electrodes: A structural and electrochemical characterization study. *Anal. Chem.* **2012**, *84*, 5823–5831. [CrossRef] [PubMed]
47. Valentini, F.; Roscioli, D.; Carbone, M.; Conte, V.; Floris, B.; Bauer, E.M.; Ditaranto, N.; Sabbatini, L.; Caponetti, E.; Chillura-Martino, D. Graphene and ionic liquids new gel paste electrodes for caffeic acid quantification. *Sens. Actuat. B Chem.* **2015**, *212*, 248–255. [CrossRef]
48. Valentini, F.; Carbone, M.; Palleschi, G. Graphene oxide nanoribbons (GNO), reduced graphene nanoribbons (GNR), and multilayers of oxidized graphene functionalized with ionic liquids (GO-IL) for assembly of miniaturized electrochemical devices. *Anal. Bioanal. Chem.* **2013**, *405*, 3449–3474. [CrossRef]
49. Han, T.-H.; Kim, H.; Kwon, S.-J.; Lee, T.-W. Graphene-based flexible electronic devices. *Mater. Sci. Eng. R Rep.* **2017**, *118*, 1–43. [CrossRef]
50. Lee, S.-M.; Kim, J.-H.; Ahn, J.-H. Graphene as a flexible electronicmaterial: Mechanical limitations by defectformation and efforts to overcome. *Mater. Today* **2015**, *18*, 336–344. [CrossRef]
51. Petrone, N.; Meric, I.; Chari, T.; Shepard, K.L.; Hone, J. Graphene Field-Effect Transistors for Radio-Frequency Flexible Electronics. *IEEE J. Electron Devices Soc.* **2015**, *3*, 44–48. [CrossRef]
52. Carbone, M.; Missori, M.; Micheli, L.; Tagliatesta, P.; Bauer, E.M. NiO pseudocapacitance and optical properties: Does the shape win? *Materials* **2020**, *13*, 1417. [CrossRef] [PubMed]
53. Guillén, C.; Herrero, J. Influence of Acceptor Defects on the Structural, Optical and Electrical Properties of Sputtered NiO Thin Films. *Phys. Status Solidi A* **2021**, *218*, 2100237. [CrossRef]
54. Mallick, G.; Labh, J.; Giri, L.; Pandey, A.C.; Karna, S.P. Facile synthesis and electron transport properties of NiO nanostructures investigated by scanning tunneling microscopy. *AIP Adv.* **2017**, *7*, 085007. [CrossRef]

55. Kwon, U.; Kim, B.-G.; Nguyen, D.C.; Park, J.-H.; Ha, N.Y.; Kim, S.-J.; Ko, S.H.; Lee, S.; Lee, D.; Park, H.J. Solution-Processible Crystalline NiO Nanoparticles for HighPerformance Planar Perovskite Photovoltaic Cells. *Sci. Rep.* **2016**, *6*, 30759. [CrossRef] [PubMed]
56. Donia, D.; Bauer, E.M.; Missori, M.; Roselli, L.; Cecchetti, D.; Tagliatesta, P.; Gontrani, L.; Carbone, M. Room Temperature Syntheses of ZnO and Its Structure. *Symmetry* **2021**, *13*, 733. [CrossRef]
57. Donia, D.T.; Carbone, M. Fate of the nanoparticles in environmental cycles. *Int. J. Environ. Sci. Technol.* **2019**, *16*, 583–600. [CrossRef]
58. Carbone, M. Cu-Zn-Co nanosized mixed oxides prepared from hydroxycarbonate precursors. *J. Alloys Compd.* **2016**, *688*, 202–209. [CrossRef]
59. Carbone, M.; Nesticò, A.; Bellucci, N.; Micheli, L.; Palleschi, G. Enhanced performances of sensors based on screen printed electrodes modified with nanosized NiO particles. *Electrochim. Acta* **2017**, *246*, 580–587. [CrossRef]
60. Carbone, M.; Briancesco, R.; Bonadonna, L. Antimicrobial power of Cu/Zn mixed oxide nanoparticles to Escherichia coli. *Environ. Nanotech. Monitor. Manag.* **2017**, *7*, 97–102. [CrossRef]
61. Carbone, M. Zn defective $ZnCo_2O_4$ nanorods as high capacity anode for lithium ion batteries. *J. Electroanal. Chem.* **2018**, *815*, 151–157. [CrossRef]
62. Carbone, M.; Sabbatella, G.; Antonaroli, S.; Remita, H.; Orlando, V.; Biagioni, S.; Nucara, A. Exogenous control over intracellular acidification: Enhancement via proton caged compounds coupled to gold nanoparticles. *Biochim. Biophys. Acta Gen.-Subj.* **2015**, *1850*, 2304–2307. [CrossRef] [PubMed]
63. Sabbatella, G.; Antonaroli, S.; Diociauti, M.; Nucara, A.; Carbone, M. Synthesis of proton caged disulphide compounds for gold nanoparticle functionalization. *New J. Chem.* **2015**, *39*, 2489–2496. [CrossRef]
64. Carbone, M.; Bauer, E.M.; Micheli, L.; Missori, M. NiO morphology dependent optical and electrochemical properties. *Colloids Surf. A* **2017**, *532*, 178–182. [CrossRef]
65. Nakate, U.T.; Ahmad, R.; Patil, P.; Yud, Y.T.; Hahn, Y.-B. Ultra thin NiO nanosheets for high performance hydrogen gas sensor device. *Appl. Surf. Sci.* **2020**, *506*, 144971. [CrossRef]
66. Carbone, M.; Tagliatesta, P. NiO grained-flowers and nanoparticles for ethanol sensing. *Materials* **2020**, *13*, 1880. [CrossRef] [PubMed]
67. Mokoena, T.P.; Swart, H.C.; Motaung, D.E. A review on recent progress of p-type nickel oxide based gas sensors: Future perspectives. *J. Alloys Compd.* **2019**, *805*, 267–294. [CrossRef]
68. Carbone, M. CQDs@NiO: An efficient tool for CH_4 sensing. *Appl. Sci.* **2020**, *10*, 6251. [CrossRef]
69. Dhas, S.D.; Maldar, P.S.; Patil, M.D.; Nagare, A.B.; Waikar, M.R.; Sonkawade, R.G.; Moholkar, A.V. Synthesis of NiO nanoparticles for supercapacitor application as an efficient electrode material. *Vacuum* **2020**, *181*, 109646. [CrossRef]
70. Xiong, S.; Jiang, S.; Wang, J.; Lin, H.; Lin, M.; Weng, S.; Liu, S.; Jiao, Y.; Xu, Y.; Chen, J. A high-performance hybrid supercapacitor with NiO derived NiO@Ni-MOF composite electrodes. *Electrochim. Acta* **2020**, *340*, 135956. [CrossRef]
71. Xiao, H.; Yao, S.; Liu, H.; Qu, F.; Zhang, X.; Wun, X. NiO nanosheet assembles for supercapacitor electrode materials. *Progr. Nat. Sci.* **2016**, *26*, 271–275. [CrossRef]
72. Di Girolamo, D.; Di Giacomo, F.; Matteocci, F.; Marrani, A.G.; Dini, D.; Abate, A. Progress, highlights and perspectives on NiO in perovskite photovoltaics. *Chem. Sci.* **2020**, *11*, 7746–7759. [CrossRef] [PubMed]
73. Guo, T.; Zhang, Z.; Yu, L.; Yuan, H.; Zhang, J.; Liu, X.; Hu, Z.; Zhu, Y. Synthesis of well dispersed NiO ink for efficient perovskite solar cells. *J. Alloys Compd.* **2021**, *860*, 157889. [CrossRef]
74. Ielmini, D.; Nardi, F.; Cagli, C. Physical models of size-dependent nanofilament formation and rupture in NiO resistive switching memories. *Nanotechnology* **2011**, *22*, 254022. [CrossRef] [PubMed]
75. Ielmini, D.; Nardi, F.; Cagli, C.; Lacaita, A.L. Size-Dependent Retention Time in NiO-Based Resistive-Switching Memories. *IEEE Electr. Device Lett.* **2010**, *31*, 353–355. [CrossRef]
76. Lee, E.M.; Ahn, Y.; Son, J.Y. Electric field control of magnetization reversal in conducting filament nanostructures in NiO resistive random access memory. *J. Alloys Compd.* **2020**, *840*, 155748. [CrossRef]
77. Lang, X.; Hirata, A.; Fujita, T.; Chen, M. Nanoporous metal/oxide hybrid electrodes for electrochemical supercapacitors. *Nat. Nanotechnol.* **2011**, *6*, 232–236. [CrossRef] [PubMed]
78. Kumar, P.V.; Ahamed, A.J.; Karthikeyan, M. Synthesis and characterization of NiO nanoparticles by chemical as well as green routes and their comparisons with respect to cytotoxic effect and toxicity studies in microbial and MCF-7 cancer cell models. *SN Appl. Sci.* **2019**, *1*, 1083. [CrossRef]
79. Ariyanta, H.A.; Ivandini, T.A.; Yulizar, Y. Novel NiO nanoparticles via phytosynthesis method: Structural, morphological and optical properties. *J. Mol. Struct.* **2021**, *1227*, 129543. [CrossRef]
80. Ukoba, K.O.; Eloka-Eboka, A.C.; Inambao, F.L. Review of nanostructured NiO thin film deposition using the spray pyrolysis Technique. *Renew. Sust. Energ. Rev.* **2018**, *82*, 2900–2915. [CrossRef]
81. Erlebacher, J.; Aziz, M.J.; Karma, A.; Dimitrov, N.; Sieradzki, K. Evolution of nanoporosity in dealloying. *Nature* **2001**, *45*, 451–453. [CrossRef] [PubMed]
82. Meher, S.K.; Justin, P.; Rao, G.R. Nanoscale morphology dependent pseudocapacitance of NiO: Influence of intercalating anions during synthesis. *Nanoscale* **2011**, *3*, 683. [CrossRef] [PubMed]

83. Brus, L.E. Electronic wave functions in semiconductor clusters: Experiment and theory. *J. Phys. Chem.* **1986**, *90*, 2555–2560. [CrossRef]
84. Raj, B.G.S.; Natesan, B.; Asiri, A.M.; Wu, J.J.; Anandan, S. Pseudocapacitive properties of nickel oxide nanoparticles synthesized via ultrasonication approach. *Ionics* **2019**, *26*, 953–960.
85. Sun, W.; Xiao, L.; Wu, X. Facile synthesis of NiO nanocubes for photocatalysts and supercapacitor electrodes. *J. Alloys Compd.* **2019**, *772*, 465–471. [CrossRef]
86. Vidhyadharan, B.; Zain, N.K.M.; Misnon, I.I.; Aziz, R.A.; Ismail, J.; Yusoff, M.M.; Jose, R. High performance supercapacitor electrodes from electrospun nickel oxide nanowires. *J. Alloys Compd.* **2014**, *610*, 143–150. [CrossRef]
87. Yuan, C.; Li, J.; Hou, L.; Yang, L.; Shen, L.; Zhang, X. Facile growth of hexagonal NiO nanoplatelet arrays assembled by mesoporous nanosheets on Ni foam towards high-performance electrochemical capacitors. *Electrochim. Acta* **2012**, *78*, 532–538. [CrossRef]
88. Yang, H.; Zou, J. Controllable preparation of hierarchical NiO hollow microspheres with high pseudo-capacitance. *Trans. Nonferrous Met. Soc. China* **2018**, *28*, 1808–1818. [CrossRef]
89. Xu, K.; Zou, R.; Li, W.; Xue, Y.; Song, G.; Liu, Q.; Liu, X.; Hu, J. Self-assembling hybrid NiO/Co_3O_4 ultrathin and mesoporous nanosheets into flower-like architectures for pseudocapacitance. *J. Mater. Chem. A* **2013**, *1*, 9107–9113. [CrossRef]
90. Hakamada, M.; Abe, T.; Mabuchi, M. Electrodes from carbon nanotubes/NiO nanocomposites synthesized in modified Watts bath for supercapacitors. *J. Power Sources* **2016**, *325*, 670–674. [CrossRef]
91. Wu, X.; Wang, Q.; Zhang, W.; Wang, Y.; Chen, W. Nano nickel oxide coated graphene/polyaniline composite film with high electrochemical performance for flexible supercapacitor. *Electrochim. Acta* **2016**, *211*, 1066–1075. [CrossRef]
92. Qiu, D.; Ma, X.; Zhang, J.; Lin, Z.; Zhao, B. In situ synthesis of mesoporous NiO nanoplates embedded in a flexible graphene matrix for supercapacitor electrodes. *Mater. Lett.* **2018**, *232*, 163–166. [CrossRef]
93. Ran, F.; Yang, H.; Wu, Y.; Zhao, X.; Tan, Y.; Liu, Y.; Niu, X.; Chen, Y.; Kong, L.; Kang, L. Facile preparation of porous nickel oxide membrane for flexible supercapacitors electrode via phase-separation method of polymer. *Mater. Res. Bull.* **2018**, *103*, 25–31. [CrossRef]
94. Buxton, S.; Garman, E.; Heim, K.E.; Lyons-Darden, T.; Schlekat, C.E.; Taylor, M.D.; Oller, A.R. Concise Review of Nickel Human Health Toxicology and Ecotoxicology. *Inorganics* **2019**, *7*, 89. [CrossRef]
95. Horie, M.; Stowe, M.; Tabei, M.; Kuroda, E. Metal ion release of manufactured metal oxide nanoparticles is involved in the allergic response to inhaled ovalbumin in mice. *Occup. Dis. Environ. Med.* **2016**, *4*, 17. [CrossRef]
96. Oller, A.R. Respiratory carcinogenicity assessment of soluble nickel compounds. *Environ. Health Perspect.* **2002**, *110*, 841–844. [CrossRef] [PubMed]
97. Sousa, C.A.; Soares, H.M.V.M.; Soares, E.V. Toxic effects of nickel oxide (NiO) nanoparticles on the freshwater alga Pseudokirchneriella subcapitata. *Aquat. Toxicol.* **2018**, *204*, 80–90. [CrossRef] [PubMed]
98. Qin, C.; Zheng, D.; Hu, Q.; Zhang, X.; Wang, Z.; Li, Y.; Zhu, J.; Ou, J.Z.; Yang, C.; Wang, Y. Flexible integrated metallic glass-based sandwich electrodes for high-performance wearable all-solid-state supercapacitors. *App. Mater. Today* **2020**, *19*, 100539. [CrossRef]
99. Wang, Z.F.; Zhang, X.M.; Liu, X.L.; Wang, Y.C.; Zhang, Y.G.; Li, Y.Y.; Zhao, W.M.; Qin, C.L.; Mukanova, A.; Bakenov, Z. Bimodal nanoporous NiO@Ni–Si network prepared by dealloying method for stable Li-ion storage. *J. Power Sources* **2020**, *449*, 227550. [CrossRef]
100. Wang, Z.F.; Fei, P.Y.; Xiong, H.Q.; Qin, C.L.; Zhao, W.M.; Liu, X.Z. $CoFe_2O_4$ nanoplates synthesized by dealloying method as high performance Li-ion battery anodes. *Electrochim. Acta* **2017**, *252*, 295–305. [CrossRef]
101. Zhao, F.; Zheng, D.; Liu, Y.; Pan, F.; Deng, Q.; Qin, C.; Li, Y.; Wang, Z. Flexible Co(OH)2/NiOxHy@Ni hybrid electrodes for high energy density supercapacitors. *Chem. Eng. J.* **2021**, *415*, 18871. [CrossRef]
102. Marsilia, M.; Susmel, S. Free-standing Plastic electrodes: Formulation, electrochemical characterization and application to dopamine detection. *Sensor. Actuat. B Chem.* **2018**, *255*, 1087–1096. [CrossRef]
103. Carbone, M.; Aneggi, E.; Figueredo, F.; Susmel, S. NiO-nanoflowers decorating a plastic electrode for the non-enzymatic amperometric detection of H_2O_2 in milk: Old issue, new challenge. *Food Control* **2022**, *132*, 108549. [CrossRef]
104. Kima, S.-J.; Lee, H.; Hong, S.-H. Solution-processed flexible NiO resistive random access memory device. *Solid State Electron.* **2018**, *142*, 56–61. [CrossRef]
105. Rakibuddin, M.; Shinde, M.A.; Kim, H. Sol-gel fabrication of NiO and NiO/WO_3 based electrochromic device on ITO and flexible substrate. *Ceram. Int.* **2020**, *46*, 8631–8639. [CrossRef]
106. Lee, S.J.; Lee, T.-G.; Nahm, S.; Kim, D.H.; Yang, D.J.; Han, S.H. Investigation of all-solid-state electrochromic devices with durability enhanced tungsten-doped nickel oxide as a counter electrode. *J. Alloys Compd.* **2020**, *815*, 152399. [CrossRef]
107. Appiagyei, A.B.; Banua, J.; Han, J.I. Flexible and patterned-free Ni/NiO-based temperature device on cylindrical PET fabricated by RF magnetron sputtering: Bending and washing endurance tests. *J. Ind. Eng. Chem.* **2021**, *100*, 372–382. [CrossRef]
108. Cao, B.; Yang, L.; Jiang, S.; Lin, H.; Wang, N.; Li, X. Flexible Quintuple Cation Perovskite Solar Cells with High Efficiency. *J. Mater. Chem. A* **2019**, *7*, 4960–4970. [CrossRef]
109. Jo, J.W.; Seo, M.-S.; Park, M.; Kim, J.-Y.; Park, J.S.; Han, I.K.; Ahn, H.; Jung, J.W.; Sohn, B.-H.; Ko, M.J.; et al. Improving Performance and Stability of Flexible Planar-Heterojunction Perovskite Solar Cells Using Polymeric Hole-Transport Material. *Adv. Funct. Mater.* **2016**, *26*, 4464–4471. [CrossRef]

110. Yin, X.; Chen, P.; Que, M.; Xing, Y.; Que, W.; Niu, C.; Shao, J. Highly Efficient Flexible Perovskite Solar Cells Using Solution-Derived NiO_x Hole Contacts. *ACS Nano* **2016**, *10*, 3630–3636. [CrossRef]
111. Wang, Z.; Rong, X.; Wang, L.; Wang, W.; Lin, H.; Li, X. Dual Role of Amino-Functionalized Graphene Quantum Dots in NiO_x Films for Efficient Inverted Flexible Perovskite Solar Cells. *ACS Appl. Mater. Interfaces* **2020**, *12*, 8342–8350. [CrossRef] [PubMed]
112. Rehman, S.; Bi, H. Electrodes for Flexible Integrated Supercapacitors, from Flexible Supercapacitor Nanoarchitectonics. *Scrivener Publ. LLC* **2021**, *Chapter 1*, 1–26.
113. Shi, S.; Xu, C.; Yang, C.; Li, J.; Du, H.; Li, B.; Kang, F. Flexible supercapacitors. *Particuology* **2013**, *11*, 371–377. [CrossRef]
114. Zhang, Y.-Z.; Wang, Y.; Cheng, T.; Lai, W.-Y.; Pang, H.; Huang, W. Flexible supercapacitors based on paper substrates: A new paradigm for low-cost energy storage. *Chem. Soc. Rev.* **2015**, *44*, 5181–5199. [CrossRef] [PubMed]
115. Chee, W.; Lim, H.; Zainal, Z.; Harrison, I.; Huang, N.; Andou, Y.; Chong, K.; Pandikumar, A. Electrospun nanofiber membrane as ultrathin flexible supercapacitors. *RSC Adv.* **2017**, *7*, 12033–12040. [CrossRef]
116. Zhai, S.; Jin, K.; Zhou, M.; Fan, Z.; Zhao, H.; Li, X.; Zhao, Y.; Ge, F.; Cai, Z. A novel high performance flexible supercapacitor based on porous carbonized cotton/ZnO nanoparticle/CuS micro-sphere. *Colloids Surf. A Physicochem. Eng. Asp.* **2020**, *584*, 124025. [CrossRef]
117. Khattak, A.M.; Yin, H.; Ghazi, Z.A.; Liang, B.; Iqbal, A.; Khan, N.A.; Gao, Y.; Li, L.; Tang, Z. Three dimensional iron oxide/graphene aerogel hybrids as all-solid- state flexible supercapacitor electrodes. *RSC Adv.* **2016**, *6*, 58994–59000. [CrossRef]
118. Fu, W.; Zhao, E.; Ma, R.; Sun, Z.; Yang, Y.; Sevilla, M.; Fuertes, A.B.; Magasinski, A.; Yushin, G. Anatase TiO_2 confined in carbon nanopores for high-energy Li-Ion hybrid supercapacitors operating at high rates and subzero temperatures. *Adv. Energy Mater.* **2020**, *10*, 1902993. [CrossRef]
119. Gwo-Bin, L.; Fu-Chun, H.; Chia-Yen, L.; Jiun-Jih, M. A new fabrication process for a flexible skin with temperature sensor array and its applications. *Acta Mech. Sin.* **2003**, *20*, 27–32. [CrossRef]
120. Yu, C.; Wang, Z.; Yu, H.; Jiang, H. A stretchable temperature sensor based on elastically buckled thin film devices on elastomeric substrates. *Appl. Phys. Lett.* **2009**, *95*, 141912. [CrossRef]
121. Dankoco, M.D.; Tesfay, G.Y.; Benevent, E.; Bendahan, M. Temperature sensor realized by inkjet printing process on flexible substrate. *Mater. Sci. Eng. B* **2015**, *205*, 1–5. [CrossRef]
122. Wang, H.; Zhu, B.; Ma, X.; Hao, Y.; Chen, X. Physically Transient Resistive Switching Memory Based on Silk Protein. *Small* **2016**, *12*, 2715–2719. [CrossRef] [PubMed]
123. Wang, H.; Zhu, B.; Wang, H.; Ma, X.; Hao, Y.; Chen, X. Ultra-Lightweight Resistive Switching Memory Devices Based on Silk Fibroin. *Small* **2016**, *12*, 3360–3365. [CrossRef] [PubMed]
124. Chen, Y.C.; Yu, H.C.; Huang, C.Y.; Chung, W.L.; Wu, S.L.; Su, Y.K. Nonvolatile Bio-Memristor Fabricated with Egg Albumen Film. *Sci. Rep.* **2014**, *5*, 1002201–1002212. [CrossRef] [PubMed]
125. Wu, Q.; Banerjee, W.; Cao, J.; Ji, Z.; Li, L.; Liu, M. Improvement of durability and switching speed by incorporating nanocrystals in the HfO_x based resistive random access memory devices. *Appl. Phys. Lett.* **2018**, *113*, 023105. [CrossRef]
126. Hu, Q.; Park, M.R.; Abbas, H.; Kang, T.S.; Yoon, T.S.; Kang, C.J. Forming-free resistive switching characteristics in tantalum oxide and manganese oxide based crossbar array structure. *Microelectron. Eng.* **2018**, *190*, 7–10. [CrossRef]
127. Chen, Y.C.; Chang, Y.F.; Wu, X.; Zhou, F.; Guo, M.; Lin, C.Y.; Hsieh, C.-C.; Fowler, B.; Chang, T.-C.; Lee, J.C. Dynamic conductance characteristics in HfO_2 based resistive random access memory. *RSC Adv.* **2017**, *7*, 12984–12989. [CrossRef]
128. Seo, J.W.; Baik, S.J.; Kang, S.J.; Lim, K.S. Characteristics of ZnO thin film for the resistive random access memory. *MRS Online Proc. Libr. Arch.* **2010**, *1250*. [CrossRef]
129. Mondal, S.; Chueh, C.-H.; Pan, T.-M. High-Performance Flexible Ni/Sm_2O_3/ITO ReRAM Device for Low-Power Nonvolatile Memory Applications. *IEEE Electron Dev. Lett.* **2013**, *9*, 1145–1147. [CrossRef]
130. Raeis-Hosseini, N.; Rho, J. Solution-Processed Flexible Biomemristor Based on Gold-Decorated Chitosan. *ACS Appl. Mater. Interfaces* **2021**, *13*, 5445–5450. [CrossRef]
131. Li, R.; Ma, X.; Li, J.; Cao, J.; Gao, H.; Li, T.; Zhang, X.; Wang, L.; Zhang, Q.; Wang, G.; et al. Flexible and high-performance electrochromic devices enabled by self-assembled 2D TiO_2/MXene heterostructures. *Nat. Commun.* **2021**, *12*, 1587. [CrossRef] [PubMed]
132. Chi, K.; Zhang, Z.; Xi, J.; Huang, Y.; Xiao, F.; Wang, S.; Liu, Y. Freestanding Graphene Paper Supported Three-Dimensional Porous Graphene−Polyaniline Nanocomposite Synthesized by Inkjet Printing and in Flexible All-Solid-State Supercapacitor. *ACS Appl. Mater. Interfaces* **2014**, *6*, 16312–16319. [CrossRef] [PubMed]
133. Gong, X.; Zhang, L.; Huang, Y.; Wang, S.; Pan, G.; Li, L. Directly writing flexible temperature sensor with graphene nanoribbons for disposable healthcare devices. *RSC Adv.* **2020**, *10*, 22222–22229. [CrossRef]
134. Hao, C.; Wen, F.; Xiang, J.; Yuan, S.; Yang, B.; Li, L.; Wang, W.; Zeng, Z.; Wang, L.; Liu, Z.; et al. Liquid-Exfoliated Black Phosphorous Nanosheet Thin Films for Flexible Resistive Random Access Memory Applications. *Adv. Funct. Mater.* **2016**, *13*, 2448–2455. [CrossRef]
135. Aziz, T.; Wei, S.; Sun, Y.; Ma, L.-P.; Pei, S.; Dong, S.; Ren, W.; Liu, Q.; Cheng, H.-M.; Sun, D.-M. High-performance flexible resistive random access memory devices based on graphene oxidized with a perpendicular oxidation gradient. *Nanoscale* **2021**, *254*, 97–105. [CrossRef] [PubMed]
136. Shinde, M.A.; Kim, H. Flexible electrochromic device with simple solution processed stable silver nanowire based transparent conductive electrodes. *Synth. Met.* **2019**, *254*, 97–105. [CrossRef]